Supporting Information

Green oxidizer based on 1,2,3-triazole with the high oxygen balance of +23.3%: A promising replacement of amommium perchloride in solid propellants

Pinxu Zhao[a, b], Long Chen[b], Qingzhong Zhang[b], Yifei Ling[b], Qiuhan Lin[a]*, Haifeng Huang[b]*, Jun Yang[b]*

[a] School of Chemistry and Chemical Engineering, Nanjing University of Science and Technology, Xiaolingwei Road 200, Nanjing 210094, P.R. China.

[b] Key Laboratory of Fluorine and Nitrogen Chemistry and Advanced Materials, Shanghai Institute of Organic Chemistry, Chinese Academy of Sciences, Lingling Road 345, Shanghai, 200032, P.R. China.

Table of contents

1. Experimental Section

Caution! Although we have encountered no difficulties during preparation and handling of these compounds, they are potentially explosive energetic materials especially **JY-23** which is sensitive to impact and friction and should be synthesized in only small amounts. Mechanical actions of these energetic materials, involving scratching or scraping, must be avoided. Manipulations must be carried out by using appropriate standard safety precautions.

5-Nitro-2-(2-oxopropyl)- 1,2,3-triazole-4-carbonitrile (2)

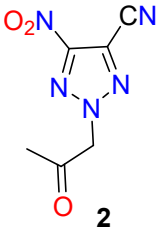

2

To the solution of 4-cyano-5-nitro-1*H*-1,2,3-triazole (**1**, 2.06 g, 14.8 mmol) in methanol was added excess solution of ammonia in methanol. After stirring at room temperature for 1 h, the solvent was removed to obtain the ammonium salt of compound 1, and then the ammonium salt was dissolved with DMF. To the solution of amonium salt of 4-cyano-5-nitro-1*H*-1,2,3-triazole in DMF (50 mL), chloroacetone (1.42 mL, 17.8 mmol) was added. Then the mixture system was heated to reflux for 12 h, and was poured into ice water. The off-white precipate (**2**) was filtered and dried by air (2.09 g). Yield: 75.0 %; ^{1}H NMR (d6-DMSO): 5.95 (s, 2H), 2.28 (s, 3H) ppm, ^{13}C NMR (d6-DMSO): 199.14, 154.13, 117.72, 109.23, 65.48, 27.10 ppm. IR (KBr): $\tilde{\nu}$ 3444, 2991, 2951, 2264, 1737, 1667, 1651, 1633, 1567, 1505, 1463, 1427, 1360, 1327, 1169, 859, 799, 767, 606, 545 cm^{-1}. HRMS (ESI) calcd for $C_6H_4O_3N_5$ [M-H]- 194.0320, found 194.0321.

(Z)-N'-hydroxy-2-((E)-2-(hydroxyimino)propyl)-5-nitro-2H-1,2,3-triazole-4-carboximidamide (3)

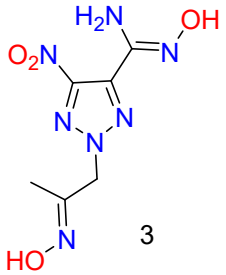

3

To the suspension of compound **2** (1.8 g, 9.2 mmol) in water (13 mL), hydroxylamine (50wt% solution, 1.65 mL, 27.12 mmol) was added dropwise. Then the mixture system was heated to reflux for 3 h and then naturally cooled to room temperature, the reaction mixture was extracted with diethyl ether (60 mL×4). The combined organic phase was dried with anhydrous magnesium sulfate. After filtration, the diethyl ether was removed at reduced pressure to obtain compound **3** as a yellow powder. (2.04 g). Yield: 90.9%; ^{1}H NMR (d6-DMSO): 11.23 (s, 1H), 9.99 (s, 1H), 6.06 (s, 2H), 5.29 (s, 2H), 1.77 (s,

3H) ppm, ^{13}C NMR (d6-DMSO): 150.08, 149.52, 142.27, 136.19, 59.66, 11.91 ppm. IR (KBr): ṽ 3500, 3439, 3396, 3265, 2139, 1650, 1574, 1556, 1525, 1425, 1381, 1362, 1295, 1254, 1171, 1129, 1039, 952, 922, 852, 814, 798, 758, 636 cm^{-1}. HRMS (ESI) calcd for $C_6H_{10}O_4N_7$ [M+H]+ 244.0789, found 244.0791.

(Z)-*N*-hydroxy-5-nitro-2-(2-oxopropyl)-1,2,3-triazole-4-carbimidoyl chloride (4)

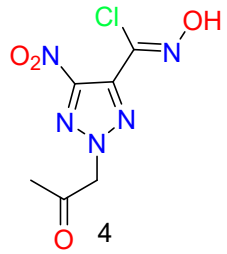

4

Compound **3** (2.0 g, 8.2 mmol) was dissolved in hydrochloric acid solution (45 mL, 20 %) at 0 °C. An aqueous solution of $NaNO_2$ (1.5 g, 8 mL) was dropped into the reaction system and the temperature was maintained at 0-5 °C for 2h, the reaction system was allowed to warm slowly up to room temperature and continued to stir for 3 h. the yellow precipitate (**4**) was collected and dried by air (1.55 g). Yield: 76.0 %;^{1}H NMR(d6-DMSO): 13.24 (s, 1H) 5.85 (s, 2H) 2.27 (s, 3H) ppm, ^{13}C NMR(d6-DMSO): 199.77, 149.34, 135.52, 123.30, 64.89, 27.11 ppm. IR (KBr): ṽ 3379, 3286, 2987, 1728, 1559, 1524, 1431, 1417, 1355, 1323, 1178, 1019, 953, 835 cm^{-1}; HRMS (ESI) calcd C6H6O4N5ClNa for [M+Na]+ 270.0001, found 270.0005.

Potassium dinitro(5-nitro-2-(2-oxopropyl)-1,2,3-triazol-4-yl)methanide (5)

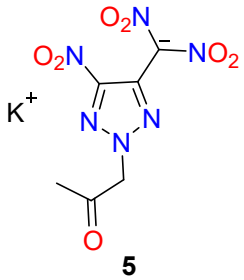

5

Compound **4** (1.02 g, 4.1 mmol) was added dropwise into a stirred mixture of trifluoroacetic acid anhydride (6.5 mL), DCM (10 mL) and fuming HNO_3 (5 mL), while maintaining the reaction temperature < 0 °C. After the addition was complete, and the mixture was maintained at 0- 5 °C. It was stirred for 30 min, and then poured into ice water (40 mL) and extracted with DCM (60 × 4 mL). The organic phases were combined, washed with water and brine, dried over sodium sulfate, and then concentrated under vacuum to provide the intermediate as a yellow oil. The oil was dissolved in methanol (60 mL), potassium iodide (1.56 g, 8.3 mmol) in methanol (13 mL) was added dropwise, and the mixture was stirred overnight at room temperature. The precipitate formed was collected by filtration and washed with methanol to give **5** as a yellow solid (863 mg) Yield: 67.0 %; ^{1}H NMR(d6-DMSO):5.78(s, 2H), 2.25(s, 3H), ^{13}C NMR(d6-DMSO): 199.89, 149.46, 136.97, 123.08, 64.59, 27.14 ppm. IR (KBr): ṽ 2986, 2939, 1735, 1563, 1526, 1463, 1414, 1369, 1323, 1223, 1185, 1146,

1040, 1015, 851, 813, 760, 750, 578, 481 cm^{-1};

4-Nitro-2,5-bis(trinitromethyl)- 1,2,3-triazole (JY-23)

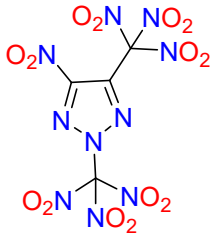

JY-23

Compound **5** (400 mg, 2.06 mmol) was dissolved in 98% sulfuric acid (6 mL) at 0 ℃ After cooling to -5 ℃, 100% nitric acid (4 mL) was added dropwise. The reaction mixture was stirred for 3 d at room temperature. Then it was poured into ice water (100 mL). The white precipitate (**JY-23**) was collected by filtration and dried by air (182 mg). Yield: 21.4 %. ^{13}C NMR($CDCl_3$): 153.3, 134.5, 119.7, 116.4 ppm. IR (KBr): ṽ 2880, 1647, 1635, 1613, 1600, 1578, 1513, 1392, 1362, 1331, 1273, 1210, 1074, 992, 942, 851, 837, 826, 791, 764, 698, 675, 648, 629 cm^{-1}; Elemental analysis: Calcd (%) for $C_4N_{10}O_{14}$ (412.14): C 11.66, H 0.00, N 33.99; Found: C 11.72, H <0.30, N 33.40.

2.X-ray Crystallographic Date

Table S1. Crystal data and structure refinement for **JY-23**.

CCDC	2256910
Empirical formula	C4 N10 O14
Formula weight	412.14
Temperature	293(2) K
Wavelength	0.71073 Å
Crystal system	Monoclinic
Space group	P 21/n
a/ Å	9.8357(6)
b/ Å	6.0788(4)
c/ Å	24.1733(15)
α(°)	90
β(°)	101.280(2)
γ(°)	90
Volume	1417.38(15) $Å^3$
Z	4
Density (calculated)	1.931 Mg/m^3
Absorption coefficient	0.197 mm^{-1}
F(000)	824
Crystal size	0.180 x 0.100 x 0.050 mm^3
Theta range for data collection	2.430 to 25.497°.
Index ranges	-11<=h<=11, -7<=k<=7, -29<=l<=28
Reflections collected	13728
Independent reflections	2626 [R(int) = 0.0584]
Completeness to theta = 25.242°	99.8 %
Absorption correction	Semi-empirical from equivalents
Max. and min. transmission	0.7456 and 0.5894
Refinement method	Full-matrix least-squares on F^2
Data / restraints / parameters	2626 / 0 / 253
Goodness-of-fit on F^2	1.042
Final R indices [I>2sigma(I)]	R1 = 0.0558, wR2 = 0.1359
R indices (all data)	R1 = 0.0851, wR2 = 0.1593

Extinction coefficient	n/a
Largest diff. peak and hole	0.354 and -0.222 e.Å^{-3}

Table S2. Atomic coordinates (x 10^4) and equivalent isotropic displacement parameters (Å^{2}x 10^3) for **JY-23**. U(eq) is defined as one third of the trace of the orthogonalized U^{ij} tensor.

	x	y	z	U(eq)
O(1)	1313(3)	5449(5)	2416(1)	85(1)
O(2)	475(2)	7764(5)	2932(1)	80(1)
O(3)	888(3)	5857(5)	4081(1)	90(1)
O(4)	721(3)	8290(5)	4708(1)	95(1)
O(5)	196(3)	11194(5)	3801(1)	89(1)
O(6)	1988(3)	11822(5)	3428(1)	84(1)
O(7)	3214(3)	12084(5)	4587(1)	95(1)
O(8)	3633(3)	8824(5)	4952(1)	88(1)
O(9)	7343(3)	8161(6)	4147(2)	108(1)
O(10)	7448(4)	4851(6)	4432(1)	116(1)
O(11)	6066(4)	7109(7)	2671(2)	121(1)
O(12)	8020(4)	6479(11)	3168(2)	194(3)
O(13)	6966(4)	2253(7)	3266(2)	131(1)
O(14)	5300(3)	2175(5)	3725(1)	92(1)
N(1)	4385(2)	7506(4)	3936(1)	54(1)
N(2)	4780(2)	6351(4)	3527(1)	55(1)
N(3)	3787(3)	5799(4)	3087(1)	56(1)
N(4)	1390(3)	6598(5)	2826(1)	61(1)
N(5)	1162(3)	7550(5)	4315(1)	64(1)
N(6)	1351(3)	10853(5)	3735(1)	65(1)
N(7)	3105(3)	10116(6)	4596(1)	69(1)
N(8)	7089(3)	6283(7)	4106(1)	72(1)
N(9)	6809(3)	6471(7)	3056(2)	85(1)
N(10)	6147(4)	3055(6)	3515(1)	78(1)
C(1)	3043(3)	7779(5)	3745(1)	50(1)
C(2)	2703(3)	6713(5)	3221(1)	50(1)
C(3)	2183(3)	9022(5)	4081(1)	55(1)
C(4)	6157(3)	5581(6)	3549(1)	60(1)

Table S3. Bond lengths [Å] and angles [°] for **JY-23**.

O(1)-N(4)	1.203(4)
O(2)-N(4)	1.211(4)
O(3)-N(5)	1.180(4)
O(4)-N(5)	1.207(4)
O(5)-N(6)	1.195(4)
O(6)-N(6)	1.213(4)
O(7)-N(7)	1.202(4)
O(8)-N(7)	1.206(4)
O(9)-N(8)	1.169(4)
O(10)-N(8)	1.181(4)
O(11)-N(9)	1.133(4)
O(12)-N(9)	1.169(4)
O(13)-N(10)	1.200(4)
O(14)-N(10)	1.185(4)
N(1)-C(1)	1.320(4)
N(1)-N(2)	1.331(4)
N(2)-N(3)	1.338(3)
N(2)-C(4)	1.424(4)
N(3)-C(2)	1.299(4)
N(4)-C(2)	1.449(4)
N(5)-C(3)	1.533(4)
N(6)-C(3)	1.530(4)
N(7)-C(3)	1.540(4)
N(8)-C(4)	1.534(4)
N(9)-C(4)	1.558(5)
N(10)-C(4)	1.537(5)
C(1)-C(2)	1.404(4)
C(1)-C(3)	1.488(4)

C(1)-N(1)-N(2)	103.0(2)
N(1)-N(2)-N(3)	116.7(2)
N(1)-N(2)-C(4)	123.9(2)
N(3)-N(2)-C(4)	119.3(3)
C(2)-N(3)-N(2)	101.6(2)
O(1)-N(4)-O(2)	125.7(3)
O(1)-N(4)-C(2)	118.4(3)

O(2)-N(4)-C(2)	115.9(3)
O(3)-N(5)-O(4)	128.3(3)
O(3)-N(5)-C(3)	116.0(3)
O(4)-N(5)-C(3)	115.8(3)
O(5)-N(6)-O(6)	128.0(3)
O(5)-N(6)-C(3)	118.3(3)
O(6)-N(6)-C(3)	113.7(3)
O(7)-N(7)-O(8)	129.4(3)
O(7)-N(7)-C(3)	117.1(3)
O(8)-N(7)-C(3)	113.5(3)
O(9)-N(8)-O(10)	129.3(4)
O(9)-N(8)-C(4)	115.3(3)
O(10)-N(8)-C(4)	115.4(4)
O(11)-N(9)-O(12)	130.9(4)
O(11)-N(9)-C(4)	116.9(3)
O(12)-N(9)-C(4)	112.1(4)
O(14)-N(10)-O(13)	128.9(4)
O(14)-N(10)-C(4)	115.2(3)
O(13)-N(10)-C(4)	115.8(4)
N(1)-C(1)-C(2)	107.6(3)
N(1)-C(1)-C(3)	120.7(3)
C(2)-C(1)-C(3)	131.8(3)
N(3)-C(2)-C(1)	111.1(3)
N(3)-C(2)-N(4)	118.9(3)
C(1)-C(2)-N(4)	129.9(3)
C(1)-C(3)-N(6)	111.8(3)
C(1)-C(3)-N(5)	112.8(3)
N(6)-C(3)-N(5)	107.9(2)
C(1)-C(3)-N(7)	110.6(2)
N(6)-C(3)-N(7)	107.2(3)
N(5)-C(3)-N(7)	106.2(3)
N(2)-C(4)-N(8)	110.0(3)
N(2)-C(4)-N(10)	109.3(3)
N(8)-C(4)-N(10)	108.8(3)
N(2)-C(4)-N(9)	112.8(3)
N(8)-C(4)-N(9)	108.1(3)
N(10)-C(4)-N(9)	107.7(3)

Symmetry transformations used to generate equivalent atoms:

Table S4. Anisotropic displacement parameters ($Å^2 x\ 10^3$) for **JY-23**. The anisotropic displacement factor exponent takes the form: $-2\pi^2[\ h^2\ a^{*2}U^{11} + ...\ + 2\ h\ k\ a^*\ b^*\ U^{12}\ ]$

	U^{11}	U^{22}	U^{33}	U^{23}	U^{13}	U^{12}
O(1)	84(2)	99(2)	59(2)	-19(2)	-14(1)	4(2)
O(2)	48(1)	112(2)	76(2)	-11(2)	0(1)	6(1)
O(3)	96(2)	78(2)	104(2)	-12(2)	43(2)	-22(2)
O(4)	86(2)	111(2)	99(2)	-14(2)	47(2)	-2(2)
O(5)	59(2)	86(2)	120(2)	-1(2)	12(2)	16(1)
O(6)	86(2)	73(2)	91(2)	16(2)	15(2)	2(1)
O(7)	92(2)	80(2)	103(2)	-29(2)	-2(2)	-12(2)
O(8)	79(2)	119(2)	57(2)	-6(2)	-3(1)	2(2)
O(9)	74(2)	106(3)	130(3)	0(2)	-14(2)	-17(2)
O(10)	110(2)	129(3)	94(2)	21(2)	-21(2)	-11(2)
O(11)	100(2)	174(4)	97(2)	44(2)	36(2)	-9(2)
O(12)	76(2)	361(8)	155(4)	75(4)	47(2)	-8(3)
O(13)	118(3)	139(3)	142(3)	-12(2)	44(2)	50(2)
O(14)	79(2)	84(2)	110(2)	20(2)	10(2)	-6(2)
N(1)	44(1)	65(2)	50(1)	-1(1)	6(1)	-5(1)
N(2)	41(1)	67(2)	54(2)	0(1)	6(1)	-1(1)
N(3)	53(2)	66(2)	47(1)	1(1)	6(1)	-2(1)
N(4)	54(2)	74(2)	50(2)	-2(1)	1(1)	-3(2)
N(5)	52(2)	76(2)	68(2)	-2(2)	18(1)	4(2)
N(6)	56(2)	60(2)	76(2)	-6(2)	4(2)	2(1)
N(7)	55(2)	88(2)	61(2)	-19(2)	5(1)	-3(2)
N(8)	48(2)	86(2)	77(2)	3(2)	2(2)	-2(2)
N(9)	46(2)	127(3)	86(2)	28(2)	20(2)	-2(2)
N(10)	62(2)	87(2)	82(2)	1(2)	7(2)	16(2)
C(1)	44(2)	57(2)	48(2)	2(1)	5(1)	-4(1)
C(2)	43(2)	58(2)	47(2)	2(1)	2(1)	-3(1)
C(3)	44(2)	63(2)	55(2)	-4(2)	5(1)	-2(1)
C(4)	44(2)	76(2)	62(2)	8(2)	9(2)	2(2)

Table S5. Torsion angles [°] for **JY-23**.

C(1)-N(1)-N(2)-N(3)	-1.6(3)
C(1)-N(1)-N(2)-C(4)	-177.7(3)
N(1)-N(2)-N(3)-C(2)	1.6(3)
C(4)-N(2)-N(3)-C(2)	178.0(3)
N(2)-N(1)-C(1)-C(2)	0.8(3)
N(2)-N(1)-C(1)-C(3)	-179.8(3)
N(2)-N(3)-C(2)-C(1)	-1.0(3)
N(2)-N(3)-C(2)-N(4)	176.4(3)
N(1)-C(1)-C(2)-N(3)	0.2(4)
C(3)-C(1)-C(2)-N(3)	-179.2(3)
N(1)-C(1)-C(2)-N(4)	-176.9(3)
C(3)-C(1)-C(2)-N(4)	3.7(6)
O(1)-N(4)-C(2)-N(3)	8.3(4)
O(2)-N(4)-C(2)-N(3)	-168.7(3)
O(1)-N(4)-C(2)-C(1)	-174.8(3)
O(2)-N(4)-C(2)-C(1)	8.2(5)
N(1)-C(1)-C(3)-N(6)	127.3(3)
C(2)-C(1)-C(3)-N(6)	-53.4(4)
N(1)-C(1)-C(3)-N(5)	-110.9(3)
C(2)-C(1)-C(3)-N(5)	68.4(4)
N(1)-C(1)-C(3)-N(7)	7.9(4)
C(2)-C(1)-C(3)-N(7)	-172.8(3)
O(5)-N(6)-C(3)-C(1)	141.7(3)
O(6)-N(6)-C(3)-C(1)	-39.8(4)
O(5)-N(6)-C(3)-N(5)	17.1(4)
O(6)-N(6)-C(3)-N(5)	-164.4(3)
O(5)-N(6)-C(3)-N(7)	-96.9(3)
O(6)-N(6)-C(3)-N(7)	81.6(3)
O(3)-N(5)-C(3)-C(1)	-21.1(4)
O(4)-N(5)-C(3)-C(1)	160.2(3)
O(3)-N(5)-C(3)-N(6)	102.9(3)
O(4)-N(5)-C(3)-N(6)	-75.9(3)
O(3)-N(5)-C(3)-N(7)	-142.4(3)
O(4)-N(5)-C(3)-N(7)	38.8(4)
O(7)-N(7)-C(3)-C(1)	109.1(3)
O(8)-N(7)-C(3)-C(1)	-70.0(4)

O(7)-N(7)-C(3)-N(6)	-13.0(4)
O(8)-N(7)-C(3)-N(6)	167.9(3)
O(7)-N(7)-C(3)-N(5)	-128.1(3)
O(8)-N(7)-C(3)-N(5)	52.7(3)
N(1)-N(2)-C(4)-N(8)	-0.1(4)
N(3)-N(2)-C(4)-N(8)	-176.2(3)
N(1)-N(2)-C(4)-N(10)	119.3(3)
N(3)-N(2)-C(4)-N(10)	-56.8(4)
N(1)-N(2)-C(4)-N(9)	-121.0(3)
N(3)-N(2)-C(4)-N(9)	63.0(4)
O(9)-N(8)-C(4)-N(2)	-70.9(4)
O(10)-N(8)-C(4)-N(2)	109.2(4)
O(9)-N(8)-C(4)-N(10)	169.4(3)
O(10)-N(8)-C(4)-N(10)	-10.5(4)
O(9)-N(8)-C(4)-N(9)	52.7(4)
O(10)-N(8)-C(4)-N(9)	-127.2(4)
O(14)-N(10)-C(4)-N(2)	-32.7(4)
O(13)-N(10)-C(4)-N(2)	145.1(3)
O(14)-N(10)-C(4)-N(8)	87.5(4)
O(13)-N(10)-C(4)-N(8)	-94.7(4)
O(14)-N(10)-C(4)-N(9)	-155.5(3)
O(13)-N(10)-C(4)-N(9)	22.3(4)
O(11)-N(9)-C(4)-N(2)	-19.6(5)
O(12)-N(9)-C(4)-N(2)	156.0(5)
O(11)-N(9)-C(4)-N(8)	-141.5(4)
O(12)-N(9)-C(4)-N(8)	34.1(6)
O(11)-N(9)-C(4)-N(10)	101.1(5)
O(12)-N(9)-C(4)-N(10)	-83.4(5)

Symmetry transformations used to generate equivalent atoms:

3. NMR Spectrum of the prepared compounds

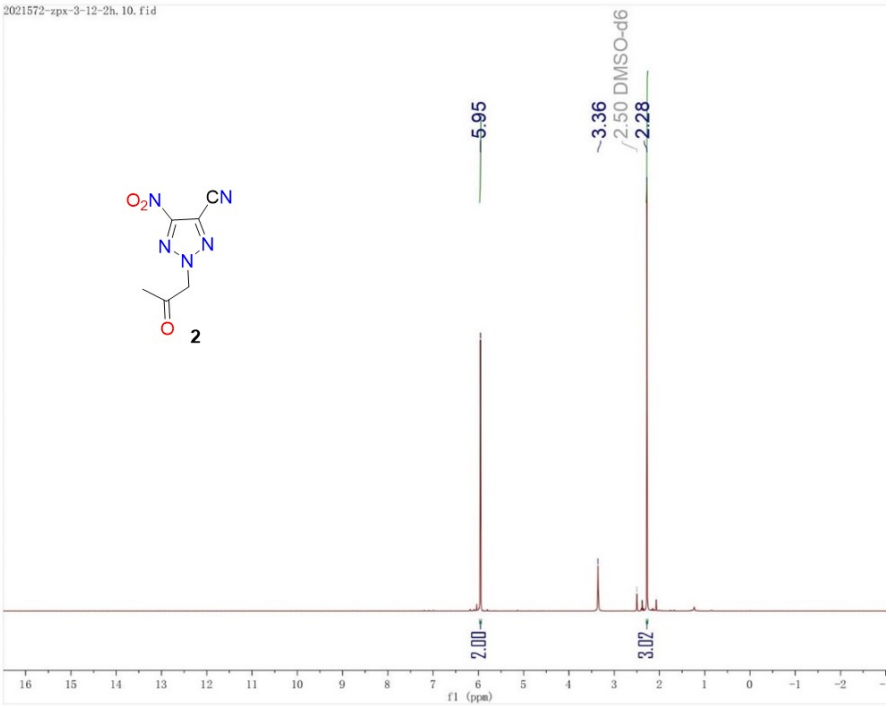

Figure S1 ^{1}H NMR spectrum of compound **2** in d_6-DMSO.

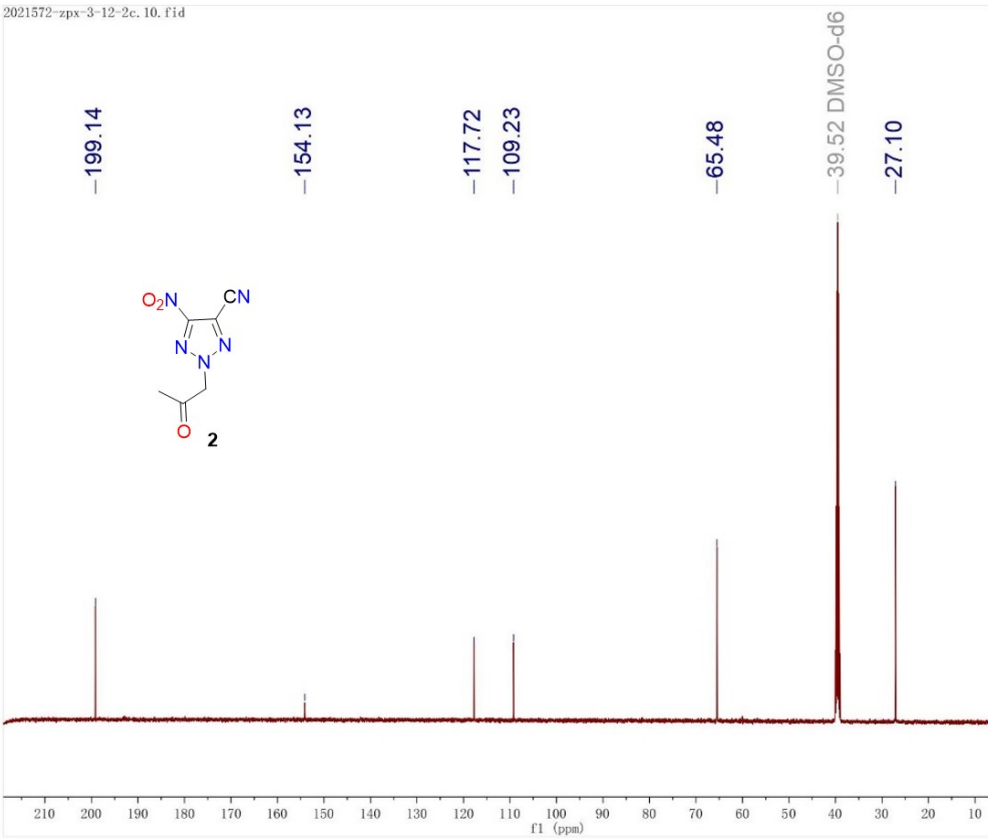

Figure S2 ^{13}C NMR spectrum of compound **2** in d_6-DMSO.

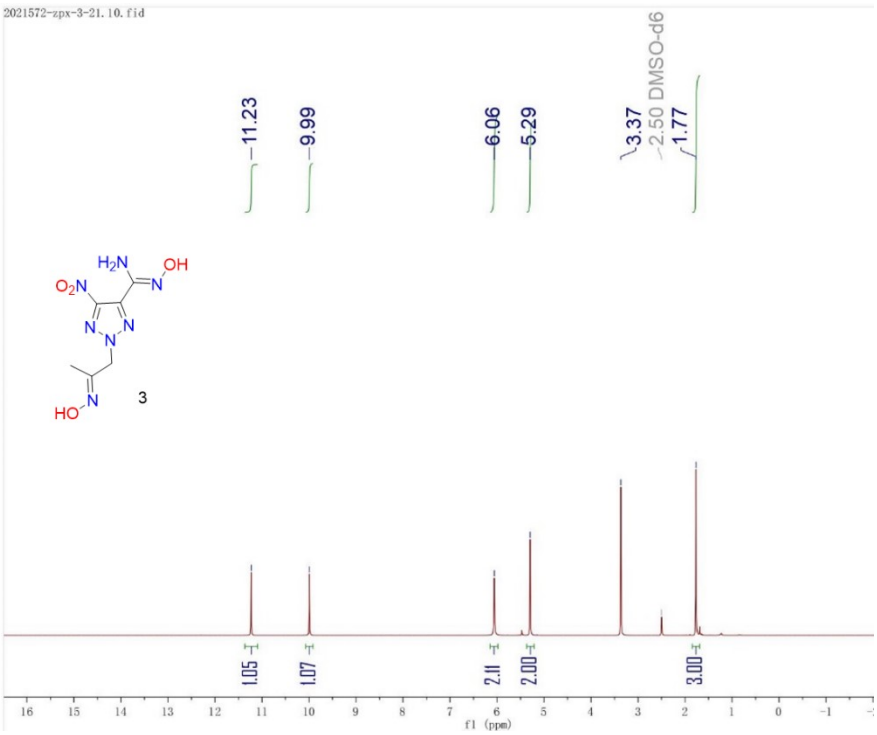

Figure S3 ^{1}H NMR spectrum of compound **3** in d_6-DMSO.

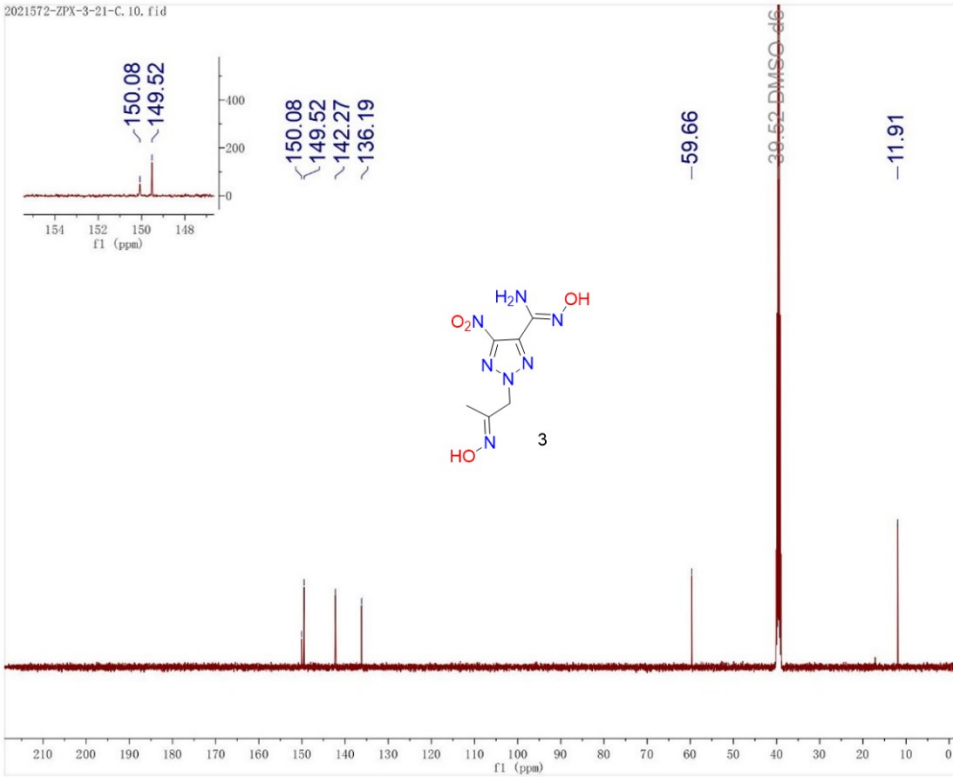

Figure S4 ^{13}C NMR spectrum of compound **3** in d_6-DMSO.

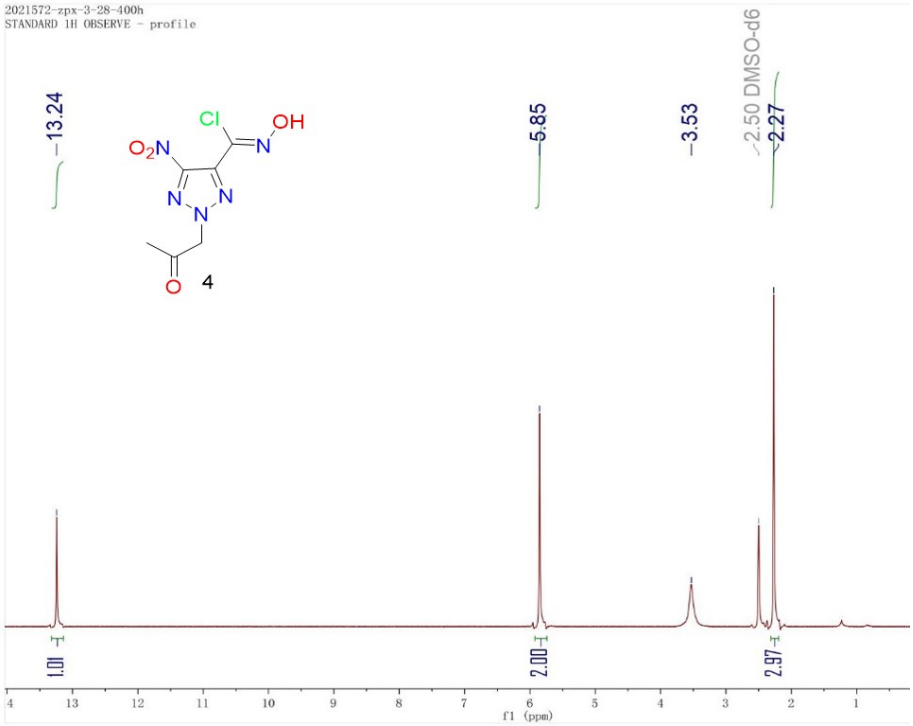

Figure S5 ^{1}H NMR spectrum of compound **4** in d_6-DMSO.

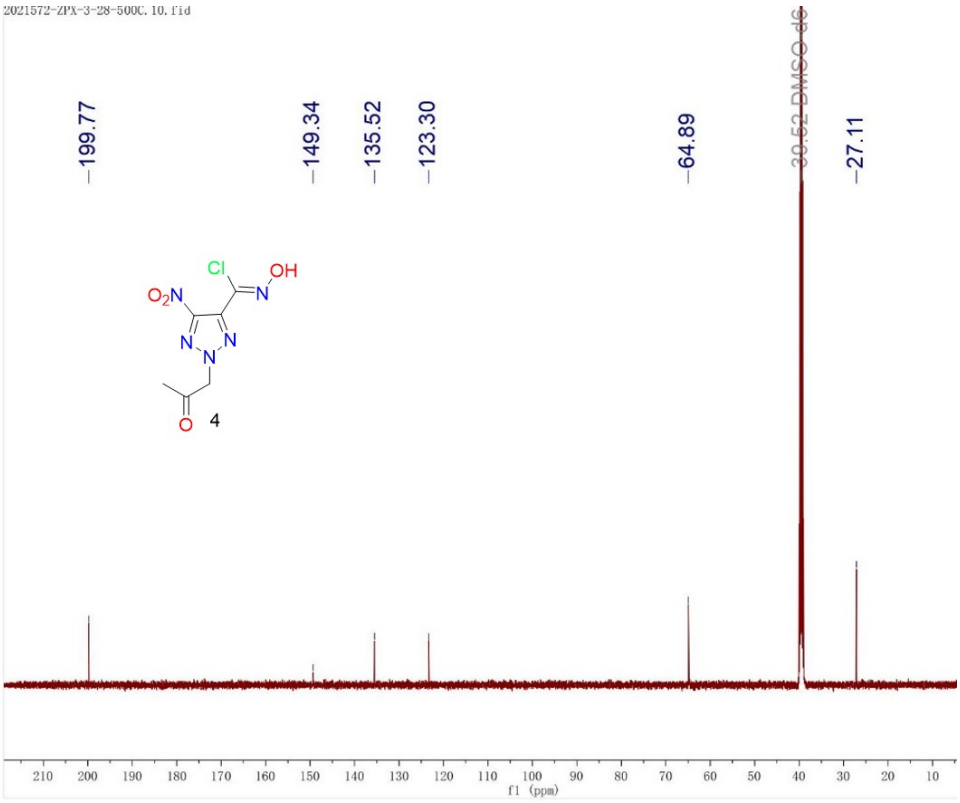

Figure S6 ^{13}C NMR spectrum of compound **4** in d_6-DMSO.

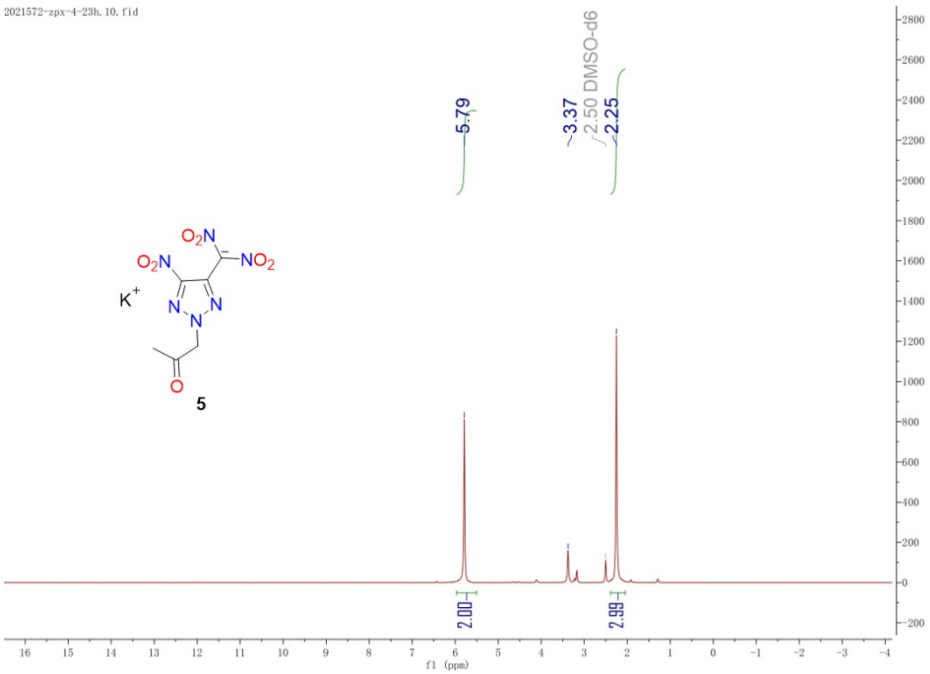

Figure S7 ^{1}H NMR spectrum of compound **5** in d_6-DMSO.

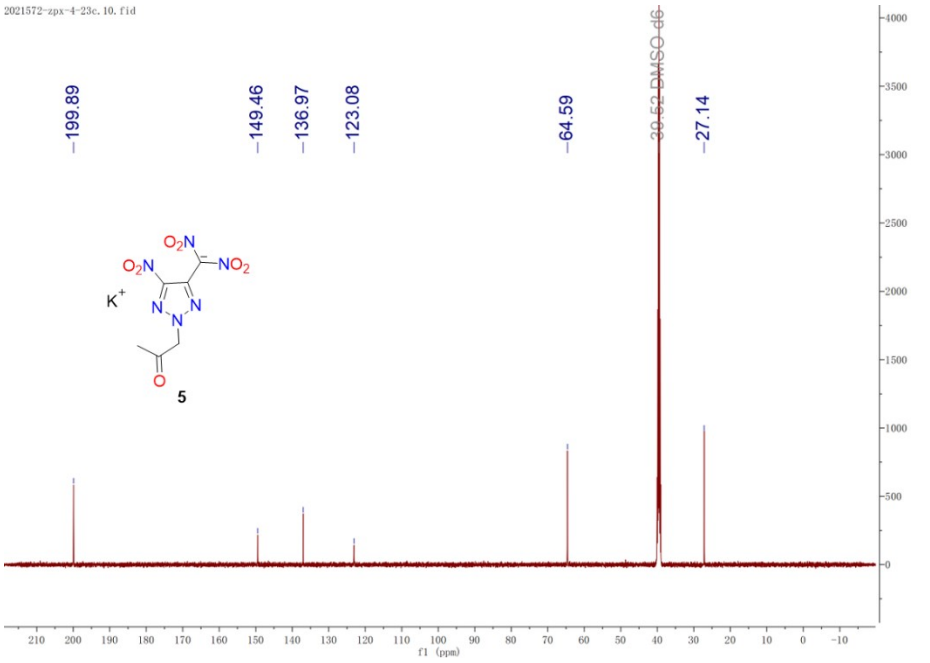

Figure S8 ^{13}C NMR spectrum of compound **5** in d_6-DMSO.

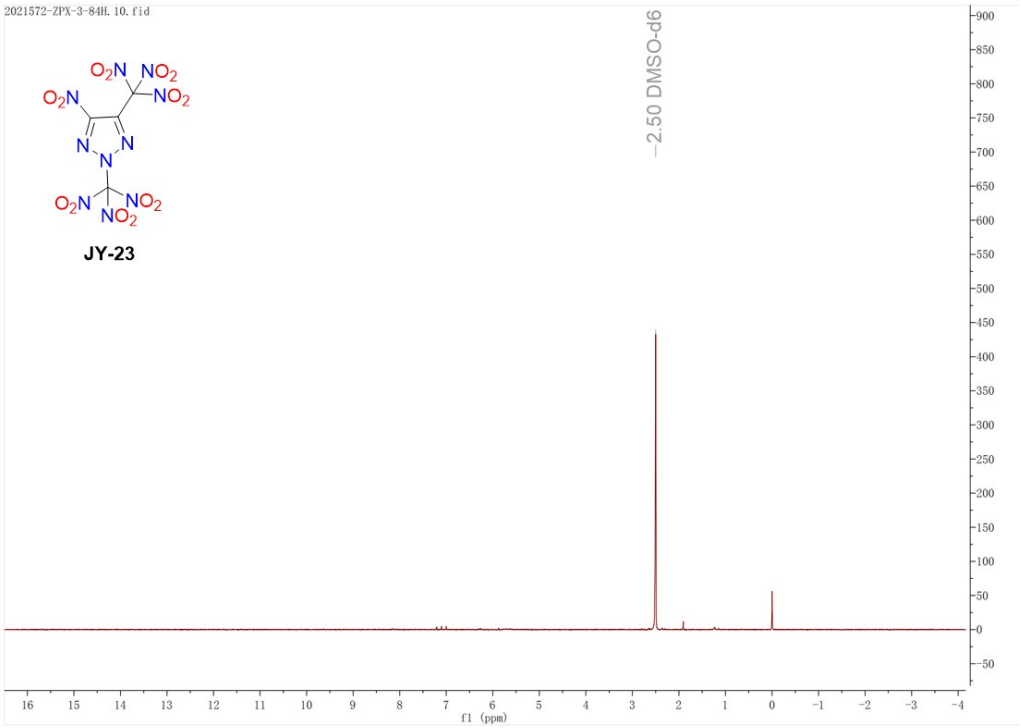

Figure S9 ^{1}H NMR spectrum of compound **JY-23** in d_6-DMSO.

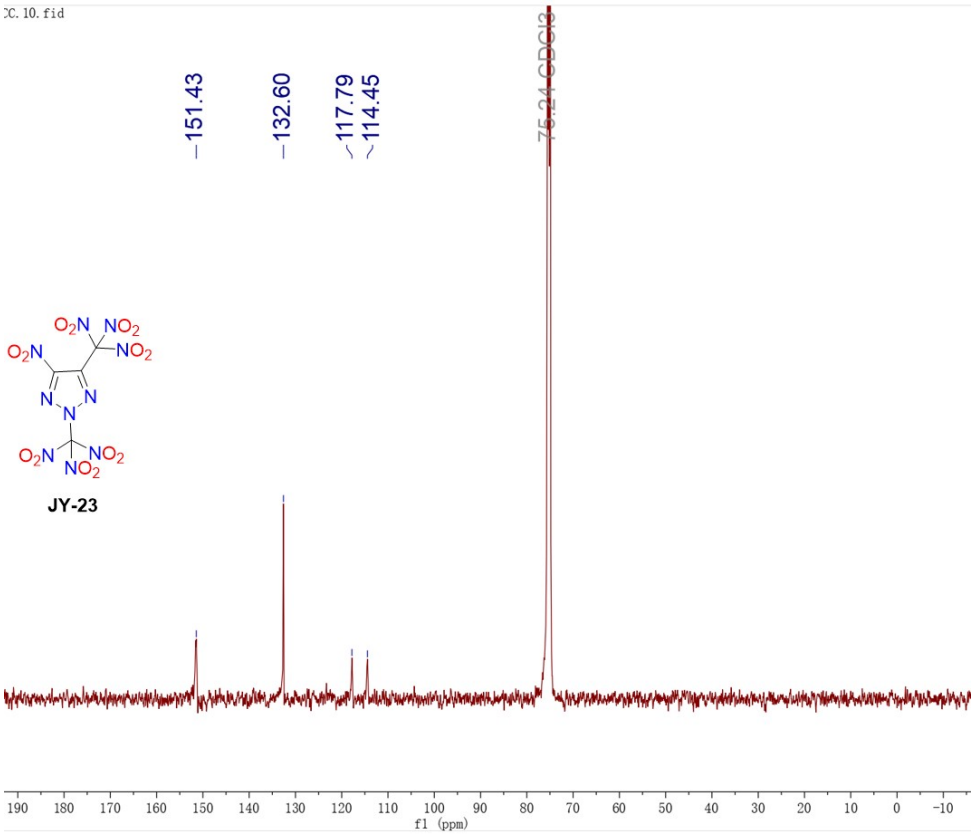

Figure S10 ^{13}C NMR spectrum of compound **JY-23** in $CDCl_3$.

4. IR Spectrum and HRMS (ESI) spectrometry of the prepared compounds

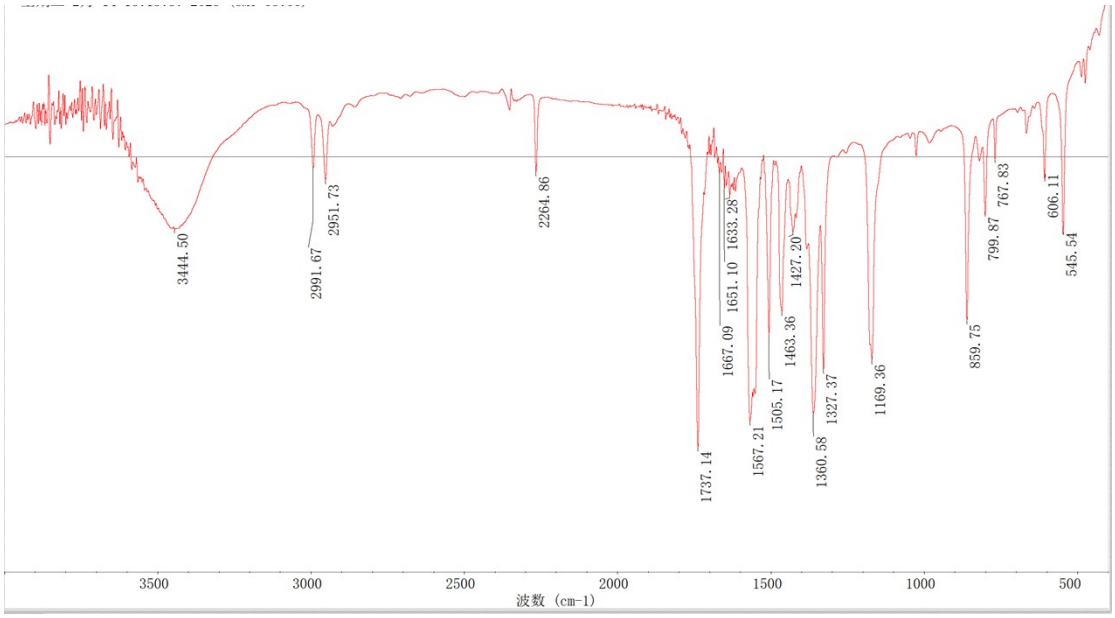

Figure S11 IR spectrum of compound **2**.

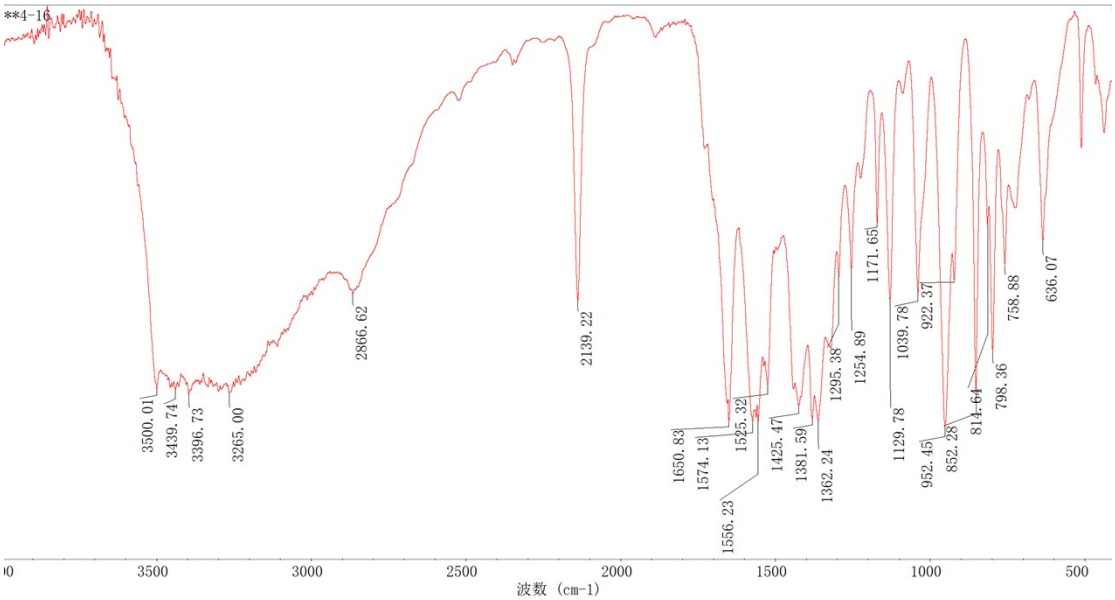

Figure S12 IR spectrum of compound **3**.

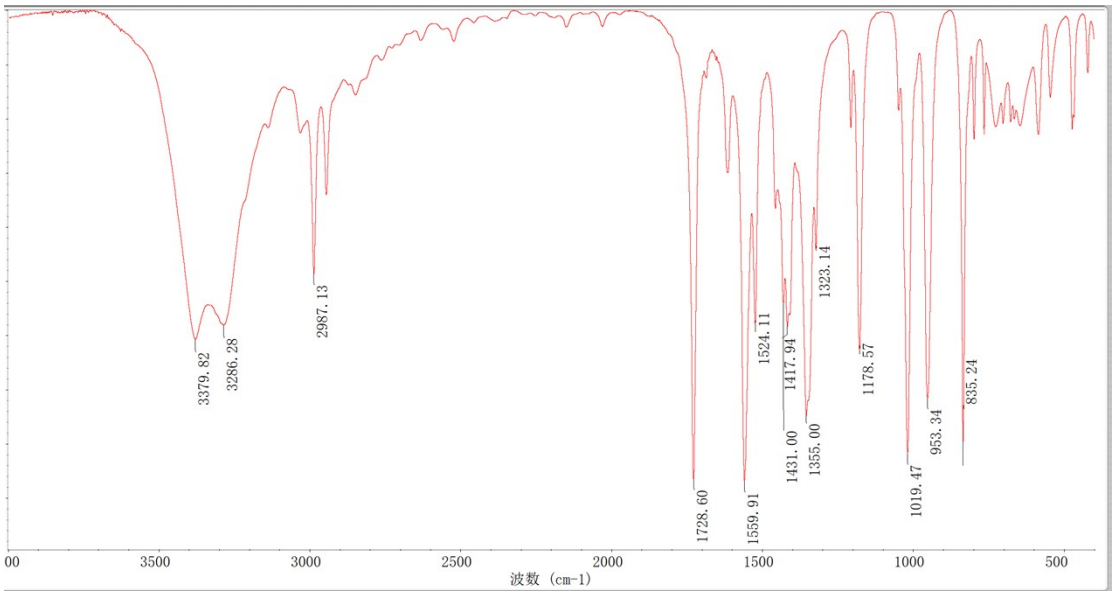

Figure S13 IR spectrum of compound **4**.

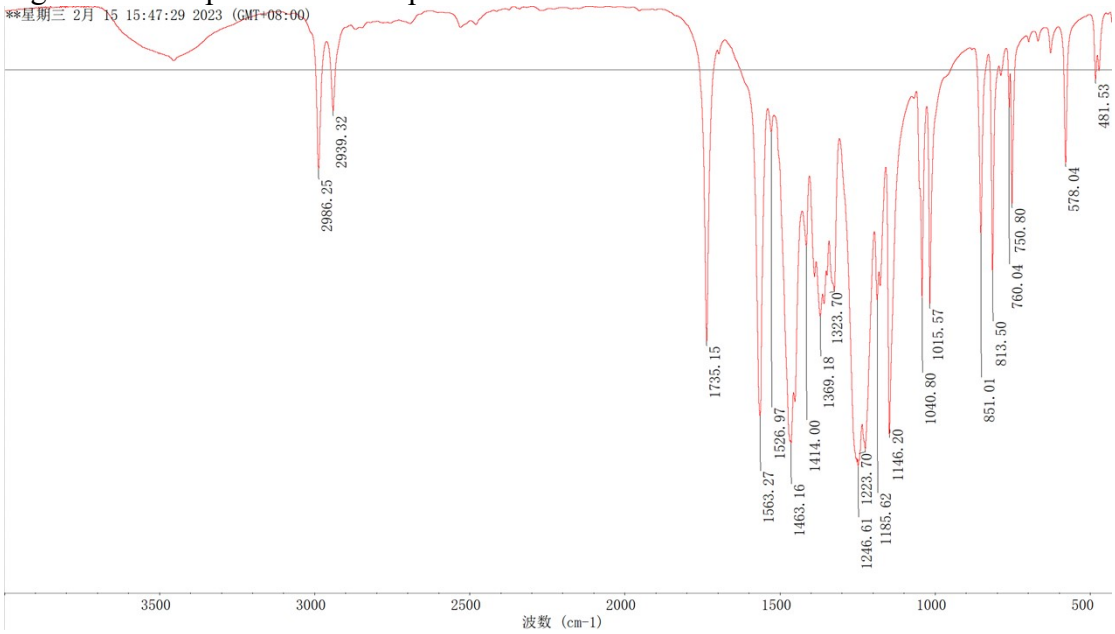

Figure S14 IR spectrum of compound **5**.

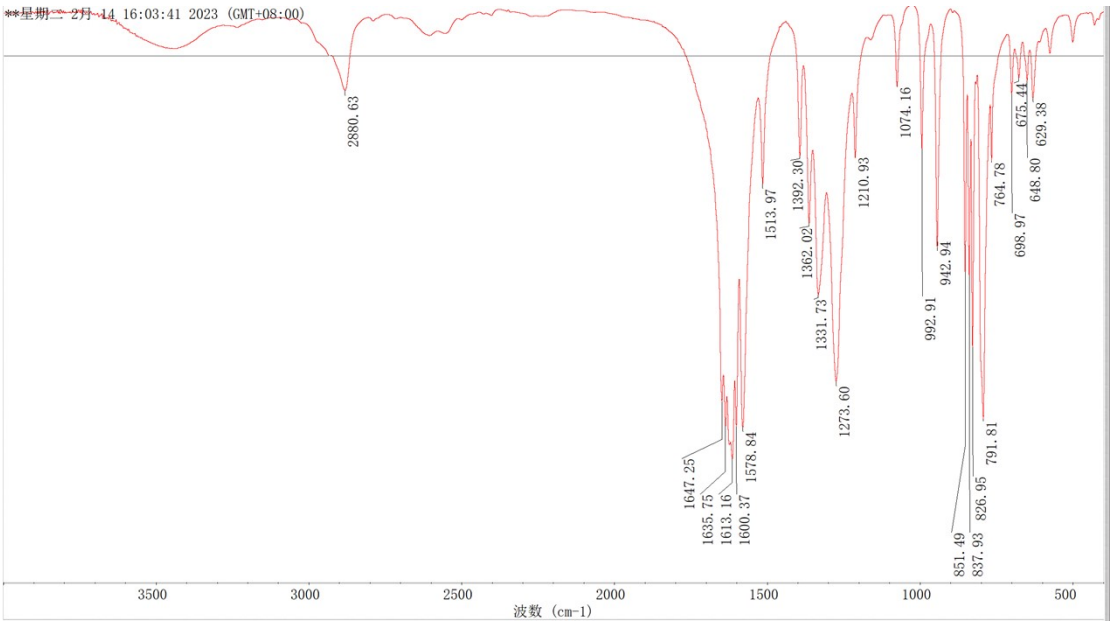

Figure S15 IR spectrum of compound **JY-23**.

National Center for Organic Mass Spectrometry in Shanghai
Shanghai Institute of Organic Chemistry
Chinese Academic of Sciences
High Resolution ESI-MS/MS REPORT

Instrument: Thermo Scientific Q Exactive HF Orbitrap-FTMS

Card Serial Number: E240294

Sample Serial Number: ZPX-5-2

Operator: Songw Date: 2024/02/02

Operation Mode: ESI Negative Ion Mode

Elemental composition search on mass 194.0321

m/z= 189.0321-199.0321

m/z	Theo. Mass	Delta (ppm)	RDB equiv.	Composition
194.0321	194.0320	0.55	7.5	$C_6H_4O_3N_5$

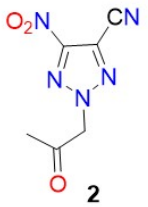

2

Figure S16 HRMS (ESI) spectrometry of compound **2**.

National Center for Organic Mass Spectrometry in Shanghai
Shanghai Institute of Organic Chemistry
Chinese Academic of Sciences
High Resolution ESI-MS/MS REPORT

Instrument: Thermo Scientific Q Exactive HF Orbitrap-FTMS

Card Serial Number: E240295

Sample Serial Number: ZPX-5-7

Operator: Songw Date: 2024/02/02

Operation Mode: ESI Positive Ion Mode

Elemental composition search on mass 244.0791

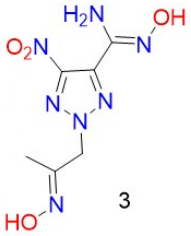

m/z= 239.0791-249.0791

m/z	Theo. Mass	Delta (ppm)	RDB equiv.	Composition
244.0791	244.0789	0.91	5.5	$C_6H_{10}O_4N_7$

Figure S17 HRMS (ESI) spectrometry of compound **3**.

National Center for Organic Mass Spectrometry in Shanghai
Shanghai Institute of Organic Chemistry
Chinese Academic of Sciences
High Resolution ESI-MS/MS REPORT

Instrument: Thermo Scientific Q Exactive HF Orbitrap-FTMS

Card Serial Number: E240302

Sample Serial Number: ZPX-5-9

Operator: Songw Date: 2024/02/02

Operation Mode: ESI Positive Ion Mode

Elemental composition search on mass 270.0005

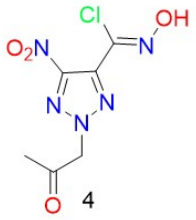

m/z= 265.0005-275.0005

m/z	Theo. Mass	Delta (ppm)	RDB equiv.	Composition
270.0005	270.0001	1.84	5.5	$C_6H_6O_4N_5ClNa$

Figure S18 HRMS (ESI) spectrometry of compound **4**.

5. TG-DSC curves and chemical stability of JY-23

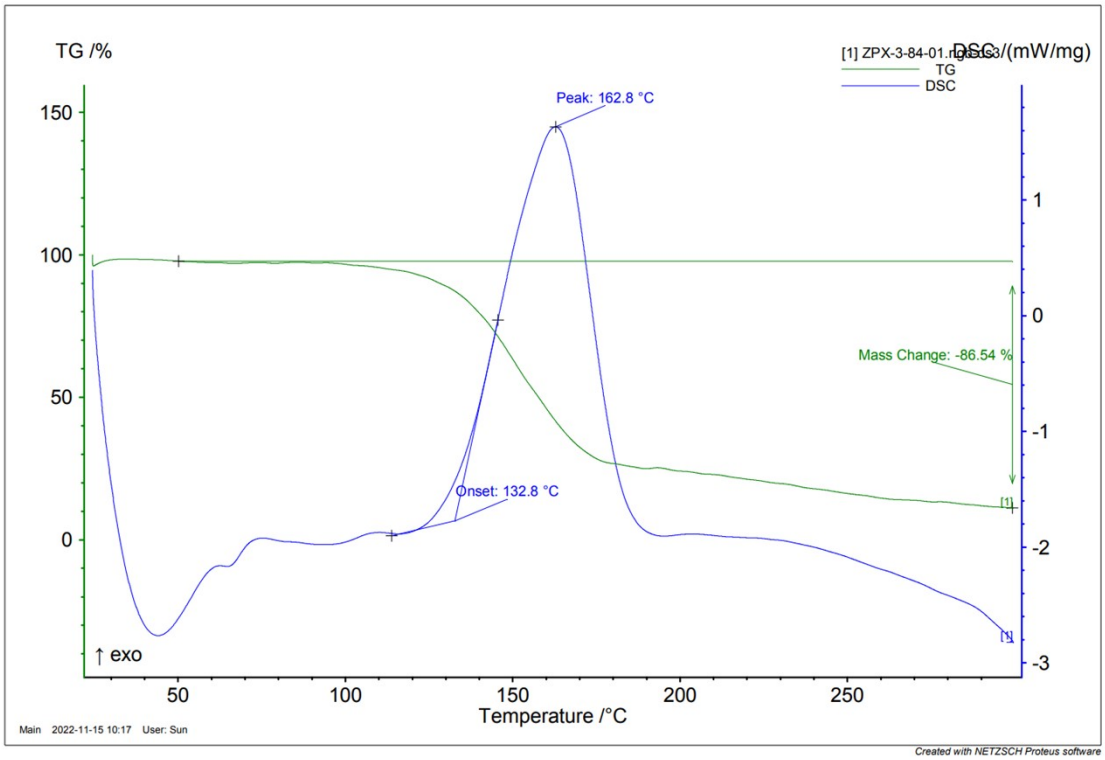

Figure S19 TG-DSC curve of **JY-23.**

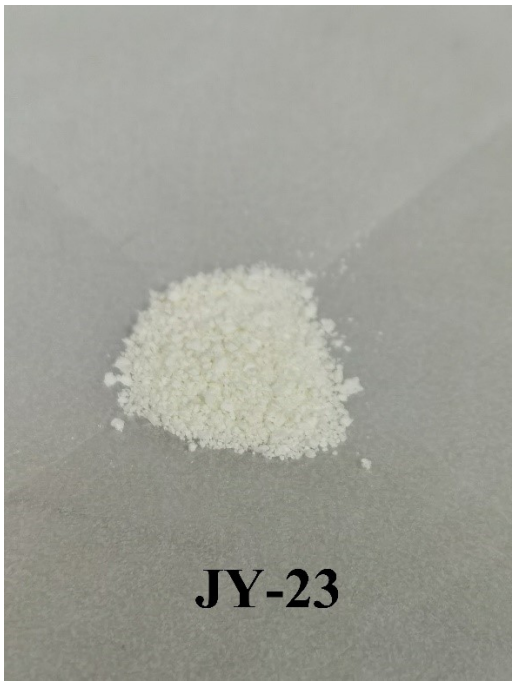

The properties of **JY-23**

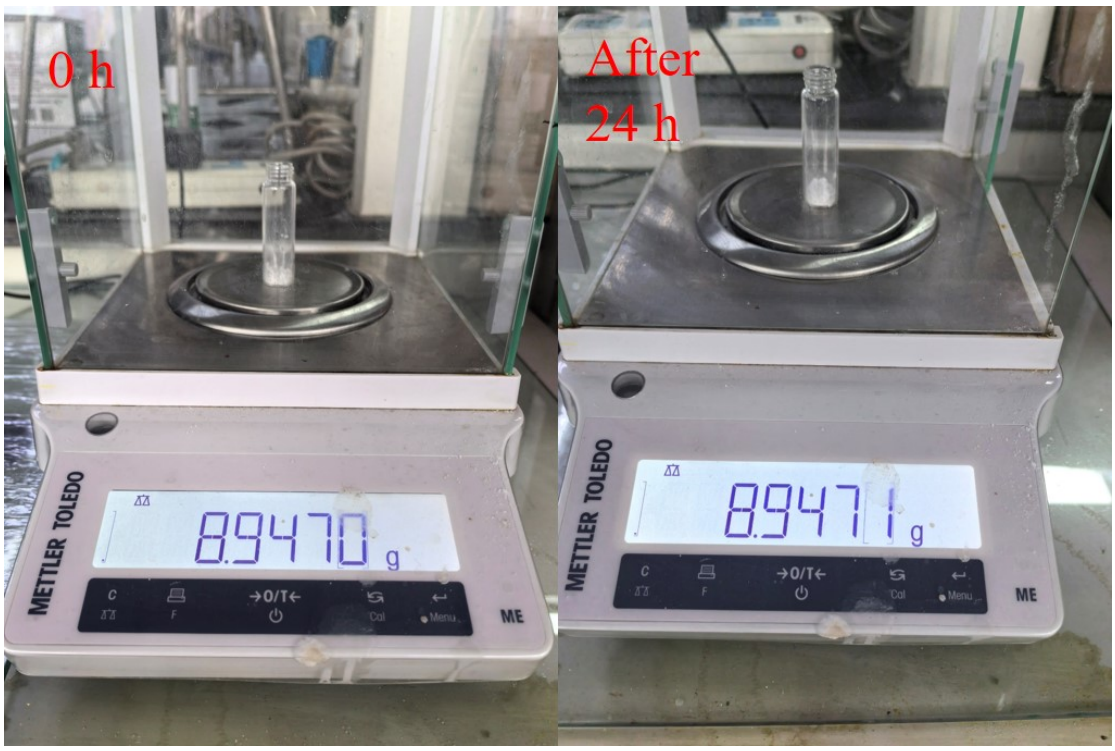

The weight monitoring of JY-23 (including bottle weight)

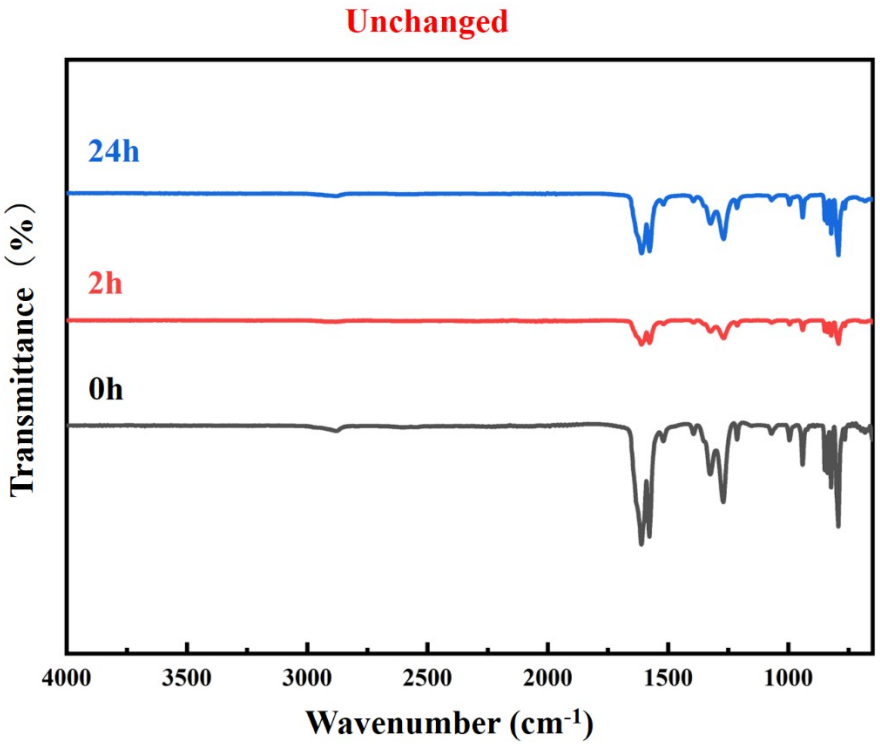

IR spectra of solid compounds exposed to air for various time periods

Figure S20 Investigation of chemical stability of **JY-23.**

6. Computations

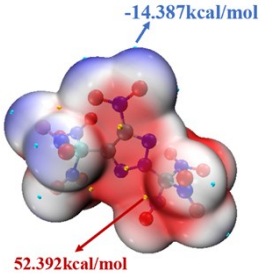

Figure S21 The electrostatic potential (ESP) on the molecular surface of **JY-23** (The geometric optimization was accomplished by using the B3LYP6-311G++(d, p) basis set.)

The G4(MP2)[1,2] method was used for calculation the enthalpy of JY-23. Calculations at the same levels of theory were performed for isolated atoms, which are used as reference for extracting the enthalpy of formation.[3] Above quantum calculations were performed using the Orca 5.0.3 [4,5] and pople python package.[6,7]

Optimized Cartesian coordinates of JY-23

C	0.47180108	-1.44356749	-0.04947104
C	0.88650591	-0.08611149	-0.04040649
N	-1.19761437	-0.22832571	-0.06645277
N	-0.83919193	-1.51050220	-0.05714622
N	-0.20016606	0.66382499	-0.04333290
C	-2.56617672	0.13690295	-0.01142239
C	2.24711180	0.51380521	-0.02278738
N	3.04113171	0.04044691	1.22967853
O	4.24033857	0.00186281	1.14963437
O	2.33341366	-0.20363563	2.18309578
N	2.15836649	2.05899718	0.06298458
O	2.42889266	2.56101147	1.12739329
O	1.80374230	2.59172728	-0.96315141
N	3.04643184	0.22137653	-1.31315475
O	2.56659221	-0.60456604	-2.06110399
O	4.06109102	0.85958407	-1.45087021
N	-2.70474299	1.67221302	0.13544148
O	-2.42133183	2.28842096	-0.86280071
O	-3.08219680	2.07395286	1.20866223
N	-3.23825890	-0.54634399	1.22779497
O	-2.51880067	-0.61801629	2.19444407
O	-4.38287661	-0.89849196	1.09304379
N	-3.36277525	-0.25599109	-1.28924763

O	-2.86367825	-1.09820750	-1.99535291
O	-4.40959202	0.33226120	-1.41829327
N	1.29004797	-2.64586955	-0.01705154
O	2.48759236	-2.44961761	0.15537281
O	0.73400306	-3.71269638	-0.15274195

The enthalpy of sublimation of JY-23 were calculated using the equation reported by Byrd and Rice.[8]

$$\Delta H_{sub} = a(SA)^2 + b\sqrt{(\sigma_{tor}^2 \nu)} + c$$

a = 0.000267, b = 1.650087, c = 2.966078

where SA is the surface area of the 0.001 electron/bohr^3 isosurface of the electron density of the molecule, σ^2_{tot} is a measure of the variability of electronic potential on the surface, and ν is the degree of balance between the positive and negative charges on the isosurface. According to ref 1, the geometry of JY-23 was optimized at B3LYP[9]/6-31G** level and the wave function analysis was conducted at B3LYP/6-311++G(2df,2p) level using Gaussian16.[x] Above parameters were obtained using Multiwfn.[10]

$$\Delta H_{solid} = \Delta H_{gas} - \Delta H_{sub}$$

Finally, based on the calculated enthalpy of formation in gaseous state and sublimation state, the enthalpy of formation in solid state of **JY-23** was estimated by subtracting the heats of sublimation from gas-phase values.

compound	ΔH_{gas}/kJ/mol	ΔH_{sub}/kcal/mol	ΔH_{solid}/kJ/mol
JY-23	437.22583	34.037673	294.81

Specific impact calculation

The energy properties of **JY-23** in HTPB and GAP propellants were studied by using NASA-CEA software at p_c = 70 atm, p_e = 1 atm, T_0 = 298 K, and compared with other heterocyclic oxidizers (**A**, **B** and **C**) in detail. I_{sp} is the theoretical specific impulse, $C*$ is the characteristic velocity, T_c is the combustion chamber temperature, M_e is the relative average molecular weight of the combustion product at the engine nozzle.

Table S6 Energy performance of AP/GAP/Al and AP/HTPB/Al propellants.

Codes	Propellant formulas	I_{sp}/N s/kg	$C*$/m/s	T_c/K	M_e	I_{sp}/s
GAP-1	$AP_{62\%}/GAP_{20\%}/Al_{18\%}$	2610.6	1584.1	3758.48	29.785	266.4
GAP-2-A	$AP_{57\%}/GAP_{20\%}/Al_{18\%}/A_{5\%}$	2616.6	1587.7	3785.41	29.895	267.0
GAP-3-A	$AP_{52\%}/GAP_{20\%}/Al_{18\%}/A_{10\%}$	2622.6	1591.3	3812.65	30.005	267.6

GAP-4-A	$AP_{47\%}/GAP_{20\%}/Al_{18\%}/A_{15\%}$	2628.6	1594.9	3840.21	30.117	268.2
GAP-5-A	$AP_{42\%}/GAP_{20\%}/Al_{18\%}/A_{20\%}$	2634.6	1598.5	3868.09	30.229	268.8
GAP-6-A	$AP_{37\%}/GAP_{20\%}/Al_{18\%}/A_{25\%}$	2640.6	1602	3896.27	30.343	269.4
GAP-7-A	$AP_{32\%}/GAP_{20\%}/Al_{18\%}/A_{30\%}$	2646.6	1605.6	3924.72	30.459	270.1
GAP-8-A	$AP_{27\%}/GAP_{20\%}/Al_{18\%}/A_{35\%}$	2652.6	1609.1	3953.32	30.577	270.7
GAP-9-A	$AP_{22\%}/GAP_{20\%}/Al_{18\%}/A_{40\%}$	2658.6	1612.6	3981.9	30.697	271.3
GAP-10-A	$AP_{17\%}/GAP_{20\%}/Al_{18\%}/A_{45\%}$	2664.4	1615.8	4010.11	30.821	271.9
GAP-11-A	$AP_{12\%}/GAP_{20\%}/Al_{18\%}/A_{50\%}$	2669.9	1618.8	4037.37	30.949	272.4
GAP-12-A	$AP_{7\%}/GAP_{20\%}/Al_{18\%}/A_{55\%}$	2674.7	1621.3	4062.73	31.082	272.9
GAP-13-A	$GAP_{20\%}/Al_{18\%}/A_{62\%}$	2677.6	1623.1	4092.36	31.278	273.2
GAP-1	$AP_{62\%}/GAP_{20\%}/Al_{18\%}$	2610.6	1584.1	3758.48	29.785	266.4
GAP-2-B	$AP_{57\%}/GAP_{20\%}/Al_{18\%}/B_{5\%}$	2614.5	1586.3	3784.69	29.938	266.8
GAP-3-B	$AP_{52\%}/GAP_{20\%}/Al_{18\%}/B_{10\%}$	2618.4	1588.5	3811.39	30.092	267.2
GAP-4-B	$AP_{47\%}/GAP_{20\%}/Al_{18\%}/B_{15\%}$	2622.3	1590.8	3838.63	30.248	267.6
GAP-5-B	$AP_{42\%}/GAP_{20\%}/Al_{18\%}/B_{20\%}$	2626.3	1593	3866.47	30.406	268.0
GAP-6-B	$AP_{37\%}/GAP_{20\%}/Al_{18\%}/B_{25\%}$	2630.2	1595.4	3894.96	30.566	268.4
GAP-7-B	$AP_{32\%}/GAP_{20\%}/Al_{18\%}/B_{30\%}$	2634.3	1597.7	3924.17	30.729	268.8
GAP-8-B	$AP_{27\%}/GAP_{20\%}/Al_{18\%}/B_{35\%}$	2638.4	1600.1	3954.12	30.894	269.2
GAP-9-B	$AP_{22\%}/GAP_{20\%}/Al_{18\%}/B_{40\%}$	2642.7	1602.5	3984.84	31.063	269.7
GAP-10-B	$AP_{17\%}/GAP_{20\%}/Al_{18\%}/B_{45\%}$	2647	1605	4016.29	31.237	270.1
GAP-11-B	$AP_{12\%}/GAP_{20\%}/Al_{18\%}/B_{50\%}$	2651.4	1607.4	4048.32	31.415	270.6
GAP-12-B	$AP_{7\%}/GAP_{20\%}/Al_{18\%}/B_{55\%}$	2655.9	1609.7	4080.6	31.59	271.0

				2	9	
GAP-13-B	$GAP_{20\%}/Al_{18\%}/B_{62\%}$	2662.1	1612.6	4125.14	31.868	271.6
GAP-1	$AP_{62\%}/GAP_{20\%}/Al_{18\%}$	2610.6	1584.1	3758.48	29.785	266.4
GAP-2-C	$AP_{57\%}/GAP_{20\%}/Al_{18\%}/C_{5\%}$	2615	1587.3	3773.23	29.778	266.8
GAP-3-C	$AP_{52\%}/GAP_{20\%}/Al_{18\%}/C_{10\%}$	2619.3	1590.4	3787.94	29.771	267.3
GAP-4-C	$AP_{47\%}/GAP_{20\%}/Al_{18\%}/C_{15\%}$	2623.6	1593.6	3802.55	29.765	267.7
GAP-5-C	$AP_{42\%}/GAP_{20\%}/Al_{18\%}/C_{20\%}$	2627.9	1596.7	3816.97	29.758	268.2
GAP-6-C	$AP_{37\%}/GAP_{20\%}/Al_{18\%}/C_{25\%}$	2632.1	1599.7	3831.07	29.752	268.6
GAP-7-C	$AP_{32\%}/GAP_{20\%}/Al_{18\%}/C_{30\%}$	2636.2	1602.6	3844.68	29.746	269.0
GAP-8-C	$AP_{27\%}/GAP_{20\%}/Al_{18\%}/C_{35\%}$	2640.1	1605.4	3857.47	29.74	269.4
GAP-9-C	$AP_{22\%}/GAP_{20\%}/Al_{18\%}/C_{40\%}$	2643.8	1608	3868.98	29.734	269.8
GAP-10-C	$AP_{17\%}/GAP_{20\%}/Al_{18\%}/C_{45\%}$	2647.1	1610.1	3878.38	29.728	270.1
GAP-11-C	$AP_{12\%}/GAP_{20\%}/Al_{18\%}/C_{50\%}$	2649.6	1611.6	3884.28	29.723	270.4
GAP-12-C	$AP_{7\%}/GAP_{20\%}/Al_{18\%}/C_{55\%}$	2650.2	1611.8	3884.21	29.72	270.4
GAP-13-C	$GAP_{20\%}/Al_{18\%}/C_{62\%}$	2635.3	1607.7	3865.96	29.729	268.9
GAP-1	$AP_{62\%}/GAP_{20\%}/Al_{18\%}$	2610.6	1584.1	3758.48	29.785	266.4
GAP-2-JY-23	$AP_{57\%}/GAP_{20\%}/Al_{18\%}/JY\text{-}23_{5\%}$	2617.6	1588.1	3789.26	29.926	267.1
GAP-3-JY-23	$AP_{52\%}/GAP_{20\%}/Al_{18\%}/JY\text{-}23_{10\%}$	2624.6	1592	3820.4	30.067	267.8
GAP-4-JY-23	$AP_{47\%}/GAP_{20\%}/Al_{18\%}/JY\text{-}23_{15\%}$	2631.6	1596	3851.95	30.209	268.5
GAP-5-JY-23	$AP_{42\%}/GAP_{20\%}/Al_{18\%}/JY\text{-}23_{20\%}$	2638.6	1600	3883.94	30.352	269.2
GAP-6-JY-23	$AP_{37\%}/GAP_{20\%}/Al_{18\%}/JY\text{-}23_{25\%}$	2645.6	1604	3916.42	30.497	267.0
GAP-7-JY-23	$AP_{32\%}/GAP_{20\%}/Al_{18\%}/JY\text{-}23_{30\%}$	2652.6	1608	3949.44	30.643	270.7

GAP-8-JY-23	$AP_{27\%}/GAP_{20\%}/Al_{18\%}/JY\text{-}23_{35\%}$	2659.7	1612	3983.01	30.792	271.4
GAP-9-JY-23	$AP_{22\%}/GAP_{20\%}/Al_{18\%}/JY\text{-}23_{40\%}$	2666.8	1616.1	4017.09	30.943	272.1
GAP-10-JY-23	$AP_{17\%}/GAP_{20\%}/Al_{18\%}/JY\text{-}23_{45\%}$	2673.9	1620	4051.61	31.099	272.8
GAP-11-JY-23	$AP_{12\%}/GAP_{20\%}/Al_{18\%}/JY\text{-}23_{50\%}$	2681.1	1623.9	4086.38	31.261	273.6
GAP-12-JY-23	$AP_{7\%}/GAP_{20\%}/Al_{18\%}/JY\text{-}23_{55\%}$	2688.3	1627.7	4121.06	31.428	274.3
GAP-13-JY-23	$GAP_{20\%}/Al_{18\%}/JY\text{-}23_{62\%}$	2697.9	1632.4	4168.47	31.674	275.3
Codes	Propellant formulas	I_{sp}/(N s/kg)	C^*/(m/s)	T_c/K	M_e	Isp/(s)
HTPB-1	$AP_{68\%}/HTPB_{14\%}/Al_{18\%}$	2601.9	1589	3383.41	25.889	265.5
HTPB-2-A	$AP_{63\%}/HTPB_{14\%}/Al_{18\%}/A_{5\%}$	2606.9	1592	3402.28	25.98	266.0
HTPB-3-A	$AP_{58\%}/HTPB_{14\%}/Al_{18\%}/A_{10\%}$	2611.6	1594.5	3419.51	26.071	266.5
HTPB-4-A	$AP_{53\%}/HTPB_{14\%}/Al_{18\%}/A_{15\%}$	2615.7	1596.5	3434.75	26.163	266.9
HTPB-5-A	$AP_{48\%}/HTPB_{14\%}/Al_{18\%}/A_{20\%}$	2618.7	1597.8	3447.55	26.255	267.2
HTPB-6-A	$AP_{43\%}/HTPB_{14\%}/Al_{18\%}/A_{25\%}$	2619.6	1598.3	3457.36	26.352	267.3
HTPB-7-A	$AP_{38\%}/HTPB_{14\%}/Al_{18\%}/A_{30\%}$	2616.3	1597.8	3463.43	26.473	267.0
HTPB-8-A	$AP_{33\%}/HTPB_{14\%}/Al_{18\%}/A_{35\%}$	2609.3	1596.1	3464.61	26.601	266.3
HTPB-9-A	$AP_{28\%}/HTPB_{14\%}/Al_{18\%}/A_{40\%}$	2599.5	1592.9	3458.96	26.719	265.3
HTPB-10-A	$AP_{23\%}/HTPB_{14\%}/Al_{18\%}/A_{45\%}$	2586.7	1587.2	3443.22	26.832	263.9
HTPB-11-A	$AP_{18\%}/HTPB_{14\%}/Al_{18\%}/A_{50\%}$	2570.1	1577.2	3412.69	26.932	262.3
HTPB-12-A	$AP_{13\%}/HTPB_{14\%}/Al_{18\%}/A_{55\%}$	2553.3	1561.6	3363.31	27.009	260.5
HTPB-13-A	$AP_{8\%}/HTPB_{14\%}/Al_{18\%}/A_{60\%}$	2537.2	1541	3295.17	27.085	258.9
HTPB-14-A	$HTPB_{14\%}/Al_{18\%}/A_{68\%}$	2514.4	1502.9	3158.1	27.209	256.6
HTPB-1	$AP_{68\%}/HTPB_{14\%}/Al_{18\%}$	2601.9	1589	3383.4	25.88	265.5

				1	9	
HTPB-2-B	$AP_{63\%}/HTPB_{14\%}/Al_{18\%}/B_{5\%}$	2605.2	1591	3403.07	26.013	265.8
HTPB-3-B	$AP_{58\%}/HTPB_{14\%}/Al_{18\%}/B_{10\%}$	2608.3	1592.6	3421.76	26.138	266.2
HTPB-4-B	$AP_{53\%}/HTPB_{14\%}/Al_{18\%}/B_{15\%}$	2611	1593.9	3439.29	26.264	266.4
HTPB-5-B	$AP_{48\%}/HTPB_{14\%}/Al_{18\%}/B_{20\%}$	2613.1	1594.8	3455.43	26.391	266.6
HTPB-6-B	$AP_{43\%}/HTPB_{14\%}/Al_{18\%}/B_{25\%}$	2614.3	1595.3	3469.86	26.519	266.8
HTPB-7-B	$AP_{38\%}/HTPB_{14\%}/Al_{18\%}/B_{30\%}$	2613.7	1595.1	3482.12	26.653	266.7
HTPB-8-B	$AP_{33\%}/HTPB_{14\%}/Al_{18\%}/B_{35\%}$	2610	1594.2	3491.52	26.804	266.3
HTPB-9-B	$AP_{28\%}/HTPB_{14\%}/Al_{18\%}/B_{40\%}$	2603.7	1592.3	3496.94	26.961	265.7
HTPB-10-B	$AP_{23\%}/HTPB_{14\%}/Al_{18\%}/B_{45\%}$	2595	1589.1	3496.41	27.112	264.8
HTPB-11-B	$AP_{18\%}/HTPB_{14\%}/Al_{18\%}/B_{50\%}$	2583.5	1583.5	3486.75	27.264	263.6
HTPB-12-B	$AP_{13\%}/HTPB_{14\%}/Al_{18\%}/B_{55\%}$	2566.3	1574	3463.74	27.409	261.9
HTPB-13-B	$AP_{8\%}/HTPB_{14\%}/Al_{18\%}/B_{60\%}$	2547.9	1559.7	3424.28	27.523	260.0
HTPB-14-B	$HTPB_{14\%}/Al_{18\%}/B_{68\%}$	2519.7	1529.2	3328.85	27.71	257.1
HTPB-1	$AP_{68\%}/HTPB_{14\%}/Al_{18\%}$	2601.9	1589	3383.41	25.889	265.5
HTPB-2-C	$AP_{63\%}/HTPB_{14\%}/Al_{18\%}/C_{5\%}$	2604.1	1590.4	3386.14	25.88	265.7
HTPB-3-C	$AP_{58\%}/HTPB_{14\%}/Al_{18\%}/C_{10\%}$	2606	1591.3	3386.82	25.871	265.9
HTPB-4-C	$AP_{53\%}/HTPB_{14\%}/Al_{18\%}/C_{15\%}$	2607.2	1591.5	3384.79	25.862	266.0
HTPB-5-C	$AP_{48\%}/HTPB_{14\%}/Al_{18\%}/C_{20\%}$	2607.1	1590.8	3379.24	25.854	266.0
HTPB-6-C	$AP_{43\%}/HTPB_{14\%}/Al_{18\%}/C_{25\%}$	2603.4	1588.8	3369.12	25.86	265.7
HTPB-7-C	$AP_{38\%}/HTPB_{14\%}/Al_{18\%}/C_{30\%}$	2592.6	1585.1	3353.09	25.913	264.6
HTPB-8-C	$AP_{33\%}/HTPB_{14\%}/Al_{18\%}/C_{35\%}$	2577.1	1579.4	3329.3	25.963	263.0

HTPB-9-C	$AP_{28\%}/HTPB_{14\%}/Al_{18\%}/C_{40\%}$	2557.9	1571.2	3294.81	26.01	261.0
HTPB-10-C	$AP_{23\%}/HTPB_{14\%}/Al_{18\%}/C_{45\%}$	2538.4	1558.9	3244.25	25.957	259.0
HTPB-11-C	$AP_{18\%}/HTPB_{14\%}/Al_{18\%}/C_{50\%}$	2522.1	1539.3	3170.12	25.915	257.4
HTPB-12-C	$AP_{13\%}/HTPB_{14\%}/Al_{18\%}/C_{55\%}$	2509.8	1513.4	3072.61	25.884	256.1
HTPB-13-C	$AP_{8\%}/HTPB_{14\%}/Al_{18\%}/C_{60\%}$	2501.8	1504	2968.34	25.861	255.3
HTPB-14-C	$HTPB_{14\%}/Al_{18\%}/C_{68\%}$	2493.9	1495.1	2946.42	25.829	254.5
HTPB-1	$AP_{68\%}/HTPB_{14\%}/Al_{18\%}$	2601.9	1589	3383.41	25.889	265.5
HTPB-2-JY-23	$AP_{63\%}/HTPB_{14\%}/Al_{18\%}/JY\text{-}23_{5\%}$	2608.6	1593	3409.07	26.008	266.2
HTPB-3-JY-23	$AP_{58\%}/HTPB_{14\%}/Al_{18\%}/JY\text{-}23_{10\%}$	2615	1596.7	3433.55	26.127	266.8
HTPB-4-JY-23	$AP_{53\%}/HTPB_{14\%}/Al_{18\%}/JY\text{-}23_{15\%}$	2621	1600	3456.69	26.247	267.4
HTPB-5-JY-23	$AP_{48\%}/HTPB_{14\%}/Al_{18\%}/JY\text{-}23_{20\%}$	2626.2	1602.8	3478.3	26.367	268.0
HTPB-6-JY-23	$AP_{43\%}/HTPB_{14\%}/Al_{18\%}/JY\text{-}23_{25\%}$	2630.3	1605.1	3498.1	26.489	268.4
HTPB-7-JY-23	$AP_{38\%}/HTPB_{14\%}/Al_{18\%}/JY\text{-}23_{30\%}$	2632.5	1606.8	3515.69	26.617	268.6
HTPB-8-JY-23	$AP_{33\%}/HTPB_{14\%}/Al_{18\%}/JY\text{-}23_{35\%}$	2631.9	1607.8	3530.42	26.763	268.6
HTPB-9-JY-23	$AP_{28\%}/HTPB_{14\%}/Al_{18\%}/JY\text{-}23_{40\%}$	2629	1607.9	3541.21	26.912	268.3
HTPB-10-JY-23	$AP_{23\%}/HTPB_{14\%}/Al_{18\%}/JY\text{-}23_{45\%}$	2624	1606.6	3546.29	27.056	267.8
HTPB-11-JY-23	$AP_{18\%}/HTPB_{14\%}/Al_{18\%}/JY\text{-}23_{50\%}$	2615.9	1603.1	3542.98	27.202	266.9
HTPB-12-JY-23	$AP_{13\%}/HTPB_{14\%}/Al_{18\%}/JY\text{-}23_{55\%}$	2600.9	1596.2	3528.17	27.34	265.4
HTPB-13-JY-23	$AP_{8\%}/HTPB_{14\%}/Al_{18\%}/JY\text{-}23_{60\%}$	2584.1	1585.2	3499.75	27.447	263.7
HTPB-14-JY-23	$HTPB_{14\%}/Al_{18\%}/JY\text{-}23_{68\%}$	2558.3	1560.9	3426.97	27.624	261.1

Reference:

1. L. A. Curtiss, P. C. Redfern, K. Raghavachari, Gaussian-4 theory, J. Chem. Phys. 2007, 126, 084108.

2. L. A. Curtiss, P. C. Redfern, K. Raghavachari, Gaussian-4 theory using reduced order perturbation theory, J. Chem. Phys. 2007, 127, 124105.
3. L. A. Curtiss, K. Raghavachari, P. C. Redfern, J. A. Pople, Assessment of Gaussian-2 and Density Functional Theories for the Computation of Enthalpies of Formation. J. Chem. Phys. 1997, 106, 1063-1079.
4. Neese, F. The ORCA program system, Wiley Interdiscip. Rev.: Comput. Mol. Sci. 2012, 2, Pages 73-78.
5. Neese, F. Software update: the ORCA program system, version 5.0, Wiley Interdiscip. Rev.: Comput. Mol. Sci. 2022, 12, e1606.
6. S. K. Das, S. Senthil, S. Chakraborty, R. Ramakrishnan, Pople: A toolkit for ab initio thermochemistry, 2021, https://moldis-group.github.io/pople/
7. S. K. Das, S. Chakraborty, R. Ramakrishnan, Critical benchmarking of popular composite thermochemistry models and density functional approximations on a probabilistically pruned benchmark dataset of formation enthalpies. J. Chem. Phys. 2021, 154, 044113.
8. E. F. C. Byrd, B. M. Rice, Improved Prediction of Heats of Formation of Energetic Materials Using Quantum Mechanical Calculations. J. Phys. Chem. A 2006, 110, 1005-1013.
9. P. J. Stephens, F. J. Devlin, C. F. Chabalowski, M. J. Frisch, Ab Initio calculation of vibrational absorption and circular dichroism spectra using density functional force fields. *J. Phys. Chem.* **1994**, *98*, 11623-11627.
10. T. Lu, F. Chen, Multiwfn: A multifunctional wavefunction analyzer. J. Comput. Chem. 2012, 33, 580-592.